# Architecture Selection and Optimization for Planet-Finding Interferometers

Serge Dubovitsky* and Oliver P. Lay
Jet Propulsion Laboratory, California Institute of Technology, 4800 Oak Grove Drive, Pasadena CA 91109

**ABSTRACT**

to be written

This draft contains all the technical information that will be in the final paper, but does need editing & formatting

Keywords:

## 1. INTRODUCTION

Planet finding is important. NASA Origins, ESA.
Key approaches: interferometer and coronagraph.
Interferometer has many architectures since the introduction of Bracewell. Traditionally they've been grouped according to theta^order null. Mention a few. How do you pick one.
In this paper we identify key selection criteria:

- planet signal isolation: chopping
- number of detections
- spectroscopy

and perform analysis to evaluate key architectures
that leads one to conclude that theta^2 options are simpler and better

## 2. NULLING ARCHITECTURE OPTIONS AND DEFINITIONS

Since the introduction of Bracewell interferometer (ref) numerous interferometer architectures have been proposed. Figure 1 (at end of paper currently) illustrates selected ones, although by no means all. The response of the interferometer ($R$) around the null is described by

$$R \propto (L\theta/\lambda)^p \tag{1.1}$$

where L – array length defined as the longest baseline connecting the centers of two collecting telescopes,

$\theta$ - angle on the sky, $\lambda$ – wavelength of operation, p – null order parameter of the nulling architecture.

The architectures are therefore often grouped by their null order, p (Bertrand reference). Introduction of higher null order architectures has been motivated by their wider nulls and therefore better suppression of stellar leakage.

* serge.dubovitsky@jpl.nasa.gov; phone 818 354 9796; fax 818 393 4950

Rotation of the array around the line of sight modulates the planet signal, as the planet crosses the fringes, and is used to isolate it from the background. The instrument performs synchronous detection at a multiple of the array rotation frequency and therefore suppresses noise components, except those occurring at the modulation frequency. Because the array rotation rate is slow, on the order of hours, the resultant signal modulation frequency is very low, millihertz, Most noise source have an 1/f spectral dependence and therefore have very high amplitudes at low frequencies

and therefore suppresses noise However, the rotation frequency is slow, on the order of hours, and ther In essence synchronous detection is performed at the array modulation frequency

Another key distinguishing characteristic between the architectures in Figure 1 is phase chopping. Phase chopping produces an intentional modulation of the planet signal which is used to isolate the desired planet signal from background and noise.

Array rotation is used Signal modulation and subsequent "synchronous detection" suppresses background and noise occurring at frequencies slower than the signal modulation frequency. Signal modulation by phase chopping is very similar to signal modulation by array rotation, except that phase chopping occurs at much higher frequencies, ~1 Hz vs 0.0001 Hz and therefore is much more effective at suppression of instrument background and ...

Both phase chopping and higher order nulls come at the expense of additional complexity and therefore $\theta^6$ architectures with phase chopping, although possible, are not considered or shown in Figure 1 because of their prohibitive complexity. For detailed descriptions of the architectures shown in Figure 1 please refer to the references provided in the caption.

Mention new options?

## 3. ARCHITECTURE SELECTION CRITERIA AND METHOD OF COMPARISON

The objective of our work for the past two years has been to select an optimum architecture for the Terrestrial Planet Finder interferometer. The available architectures differ in numerous ways, but we identified the following key criteria:

A) Planet signal isolation.

The detected planet photon rate is significantly below the photon rate due to other sources of emission. For example, the planet photon rate is one to two orders of magnitude below the rate of stellar photons leaking through the null, even for wide null configurations. This occurs because for the earth-like planet flux is roughly $2x10^{-7}$ of the star at 10 um while the expected null floor is $10^{-6}$. Similarly, the local zodi levels greatly exceed the detected planet photon rates (reference Oliver or later section). Signal modulation and subsequent detection at the modulation frequency therefore is required to pull the desired planet signal out of the background. Array rotation (ref) provides a method for such synchronous detection and would be entirely sufficient if all other emission sources were constant during the array rotation time of hours or days. The local zodi and exo-zodi rates should remain constant on these time scales, but detected photon rates due to internal thermal emissions, stray light, detector gain variations, and instrument instabilities will not be sufficiently constant, especially in the presence of array rotation, and will contribute noise at the signal modulation frequency. Phase chopping is a method to increase planet signal modulation frequency and moves synchronous planet detection to frequencies ~ 1 Hz, where fluctuations of other emission sources are expected to be much weaker. The modulation results from sweeping the interferometer's fringes across the sky by rephrasing the arms of the interferometer. It is the optical analogue of phased array pointing. Phase chopping enables isolation of the planet signal from other sources of emission

We therefore consider phase chopping a must for an interferometer architecture. This strong criterion eliminates a number of options listed in Fig. 1. For example, none of the $\theta^6$ configurations can support phase chopping with reasonable levels of instrument complexity. The remaining options are marked .....

B) Number of stellar systems searched for planets

It is important for an instrument to examine a statistically meaningful number of stellar systems for presence of earth-like planets in order to i) find planets if they exist or ii) provide a meaningful negative result. For example, the current TPF science requirements call for a minimum mission to search 35 stars and for full mission to search at least 165 stars. The number of searched systems becomes a key selection criterion between the remaining phase-chopping-capable architectures. The bulk of this paper, Section XX, is devoted to describing a method for calculating a number of stellar systems that can be examined during a mission lifetime for a particular architecture. This discriminator for architecture selection, instead of previously accepted "minimize the stellar leakage" guiding principle, leads to a surprising conclusion that $\theta^2$ architectures do better despite their higher stellar leakage.

C) Number of planet spectra measured

Once a planet is detected it is important to measure its spectrum in order to i) confirm a planet detection and ii) characterize a planet. The current science requirements, for example, call for measuring spectra of at least 50 % of detected planets. This translates into 1-2 planetary spectra for minimum mission and 8 for full mission. The calculation of the number of spectra that can be obtained during the mission lifetime is closely related to calculations for B) and is described in Section XX.

D) Feasibility of the beam combiner

Some architectures require extremely complex beam combiners, while others are relatively straightforward. The beam combiner designs have been considered in ref (Gene). Consideration of the beam combiner design serves as an important check on the architecture selection process and also provides efficiency numbers needed for evaluation of criteria B) and C).

### 3.1. Number of stellar systems searched for planets

The overall mission time is split between time allocated for planet detection and planet characterization phases. In addition there are inefficiencies associated with instrument operations and re-targeting. The number of stellar systems that can be searched for planets ($\mathcal{N}_d$) during a part of the mission allocated for detection is a key discriminating factor between the architectures. We calculate this number for each architecture by going through the following steps, discussed in more details below:

1) Start with a *Target* star list: a list of stars thought likely to contain planets.
2) *Eligible* stars list: Eliminate from the *Target* list stellar systems that cannot be examined because of the interferometer's engineering limitation, e.g. stars outside of the Field of Regard (FOR)

For a given array size L produce

3) *Observable* stars list: reduce the *Eligible* stars list to the stars with inner habitable zone that can be resolved by the interferometer.
4) Calculate an integration time $T_{int}(L)$ required to detect a minimum-size terrestrial planet around each of the *Observable* stars with required signal-to-noise ratio (SNR). Account for multiple visits needed for detection.
5) Order the stars in ascending order of integration time. Start with the shortest integration time star and see how many stellar systems can be consecutively searched within the allocated mission time. For a fixed length configuration, i.e. Structurally Connected Interferometer (SCI), this will be the reported number of stars searched, $\mathcal{N}_d$. These stars are stored in the *Searched* stars list.

If the configuration has a variable array length, i.e. Formation Flying Interferometer (FFI) then

6) Find the array length, subject to $L_{min}<L<L_{max}$ appropriate for a given configuration, that produces a minimum integration time for each star, $T_{int}$. In other words, assume the array will be re-sized for each star.
7) Produce an ordered list as in step 5) but using the minimum times found in 6). Start with the shortest integration time star and see how many stellar systems can be consecutively searched within the allocated mission time. This will be the reported as number of stars searched, $\mathcal{N}_d$, for a given architecture.

### 3.1.1. Target Star List

The current *Target* star list was provided by Ken Johnston of the TPF Science Working Group. It was produced by selecting the Hipparcos catalog stars within 30 parsecs (2350 stars) and applying a series of science culls.

The culls **excluded** the following stars:

i) apparent magnitude > 9th

ii) bolometric luminosity > 8th magnitude

iii) Luminosity class: I, II or III

iv) B-V index < 0.3

v) Variability > 0.1

vi) Multiple systems with companions closer than 50 AU

The remaining *Target* star list contains 1014 stars. The distribution of stellar types vs. distance in the *Target* list is shown in Figure 2.

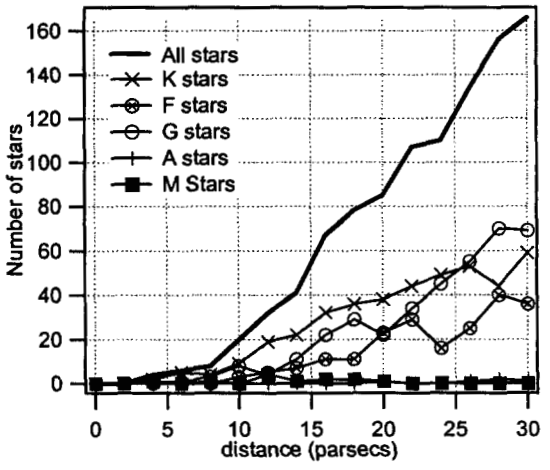


Figure 2. Statistics of the *Target* star list.

### 3.1.2. Eligible stars

The next step is to eliminate from the *Target* list stellar systems that cannot be examined because of the interferometer's engineering limitation. The two limiting factors currently accounted for are Field of Regard and stellar multiplicity

One limitation is the Field of Regard (FOR). Interferometer optics must be shielded from the sunlight at all times. Even small amounts of sunlight glare would swamp the faint planet signal and therefore large shades are deployed. The practical limitations on the size of sun shades and the telescope optics dictate that the interferometer's field of regard is limited to $\pm\theta_{FOR}$ degrees around the anti-sun direction. Assuming the spacecraft orbit the sun in the plane of the solar system the FOR limitation means that the instrument can only look at the stars with ecliptic latitude of $\pm\theta_{FOR}$ , consequently all other stars are excluded from the list. The magnitude of $\theta_{FOR}$ is primarily governed by the size of the shades and the height of the telescopes and is around 45 degrees for our current designs.

There is another effect connected to the instrument's limited FOR and the stellar ecliptic latitude: the time available to observe the star. This effect is considered in Section x.x.x.

Stellar multiplicity is another factor accounted for in the model. If a star has a companion that appears closer than $\theta_{mult}$ the star is excluded from the list, because companion would interfere with the observation of a planet. Typical value of $\theta_{mult}$ is 10 asec.

### 3.1.3. Observable stars: resolution

To search a stellar system for planets the inner-most expected angular location of the planet, $\theta_p$, must be higher than the Inner Working Angle, $\theta_{IWA}$, of the instrument.

The inner-most planet location is estimated as a fraction $X_{IHZ}$ of the expected location of an Earth-like planet given by the Earth-sun distance, $r_{Earth}$=1AU, scaled by the luminosity of the observed star, $\mathcal{L}_*$, relative to that of the sun, $\mathcal{L}_{sun}$. $X_{IHZ}$ is given by the science requirements and is currently 0.7. Because the planetary system may be inclined relative to the observation direction, an additional factor, $X_{incl}$=0.78, is used to account for the average shortening of the apparent angle due to inclination.

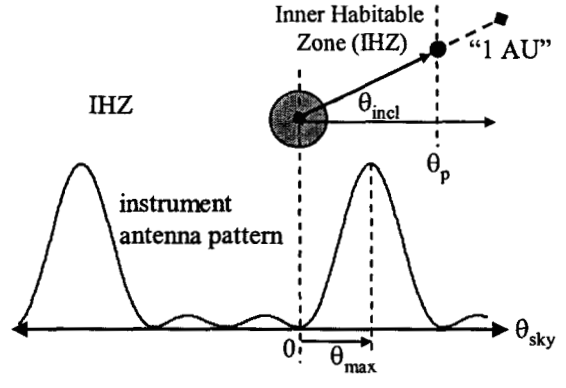


Figure 3

$$\theta_p = X_{incl} X_{IHZ} \frac{r_{Earth}\sqrt{\mathcal{L}_*/\mathcal{L}_{sun}}}{d_*} \qquad (1.2)$$

The geometry is illustrated in Figure 3. The interferometer inner working angle is defined as a fraction, or a multiple, of the first fringe maximum, $X_{IWA}$:

$$\theta_{IWA} = X_{IWA}\theta_{\max} \quad \text{and} \qquad \theta_{\max} = \chi\frac{\lambda_{res}}{L} \tag{1.3}$$

where L – array length, longest baseline connecting the centers of two collecting telescopes

$\lambda_{res}$ – resolution wavelength, 10 μm in this study

$\chi$ – configuration dependent resolution parameter, e.g. ¾ for Dual Chopped Bracewell architecture. Values for other architectures are shown in Table 1 and in ref. Charley. The smaller the number the more efficient the architecture at using the array length.

For this study value of $X_{IWA}$ =1 was used.

For each star on the *Eligible* list an expected inner most planet angle, $\theta_p$, was calculated and compared to the interferometer inner working angle, $\theta_{IWA}$, at a given L, i.e. for one particular configuration.

Stars were **excluded** from the list **if** $\theta_{IWA} > \theta_p$. The remaining stars, the ones whose planets can be resolved by the interferometer, are kept to form the *Observable* stars list

### 3.1.4. Measured stars: time

The next step is to calculate an integration time required for a given interferometer configuration to detect a planet around a star on the Observable star list.

$$T_{\text{int}} = \left(SNR_{\text{req}}/SNR_{1\text{sec}}\right)^2 \tag{1.4}$$

where $SNR_{\text{req}}$ – signal-to-noise ratio required for detection. Current TPF science requirements call for $SNR_{\text{req}}$=5.

$SNR_{1\text{sec}}$ – signal-to-noise ration obtained during one second of integration.

The $SNR_{1\text{sec}}$ based on two noise components: random photon noise and systematic instrument noise (ref. Oliver). In this study we assume that the error budget allocation will be such as to make the systematic noise roughly equal to the expected photon noise. Consequently, the $SNR_{1\text{sec}}$ obtained at single interferometer output port will be estimated by doubling the easier to calculate photon noise.

$$SNR_{1\text{sec}} = \sqrt{N_{\text{det}}}\frac{S_p}{\sqrt{2\left(S_{LZ}+S_{SL}\right)}} \tag{1.5}$$

where Sp – planet signal

$S_{LZ}$ – local zodi detected photo-electron rate

$S_{SL}$ – photo-electron rate due to stellar leakage

$N_{\text{det}}$ – number of output ports used. Should probably say something about that.

The notable absence from the above expression is the exo-zodi contribution. We have analyzed the exo-zodi contribution using a more sophisticated model, and found that a solar system level of exo-zodi emission is not a major contributor of photon noise, relative to stellar leakage and the local zodi. At dust densities of 5 times the solar system level, it does become more important, however, with a contribution that depends on distance, inclination angle and the configuration.

#### 3.1.4.1. Planet signal

The planet signal is given by

$$S_p = \tfrac{1}{2}\eta_{\text{mod}}\tau A_{tot}\Omega_p\int_{\nu_1}^{\nu_2}B_{ph}\left(\nu,T_p\right)d\nu \tag{1.6}$$

where $\eta_{\text{mod}}$-modulation efficiency of a given interferometer architecture. The values are listed in Table 1 and discussed below.

$\tau$ – internal throughput of the instrument. Includes optics losses and detector conversion efficiency.

$A_{\text{tot}}$ – total collecting area of the instrument

$\Omega_p = \pi\left(\frac{R_p}{d_*}\right)^2$ – solid angle subtended by the planet

$R_p$ – planet radius

$d_*$ - distance to the star

$B_{ph}(\nu,T)=\frac{2}{c^2}\frac{\nu^2}{\left[\exp\left(\frac{h\nu}{kT}\right)-1\right]}$ - Plank's distribution function in units of photons/m$^2$/sec/Hz/sr (check???? Look up in Zombek proper name for this function) (1.7)

factor of ½ occurs in front because this is the signal out of one port. In a chopped configuration a single port looks at the planet only during half the time.

$\nu_1$, $\nu_1$ - frequencies corresponding to the end points of a given optical bandwidth channel , $\nu_{1,2}=c/\lambda_{1,2}$ .

The modulation efficiency for an array, $\eta_{mod}$, is a measure of how efficiently a nulling configuration generates modulated planet output, relative to the total collecting area. Six steps are needed to derive this number: (1) calculate the antenna response on the sky for each of the two phase chop states; (2) take the difference in the antenna responses for the two chop states to obtain the chopped antenna; (3) generate the time-varying chopped planet output photon rate that results as the array is rotated, and the chopped antenna response sweeps over the planet; (4) calculate the root-mean-square (rms) of this chopped planet output; (5) normalize by dividing out the planet flux, total collecting area and instrument throughput; (6) repeat steps 3 to 5 for different angular offsets of the planet from the star; and (6) fit an average level to this angular dependence to obtain the modulation efficiency, excluding the central null, which lies inside the inner working angle. An example of the last two steps is shown in Fig. 4 for a standard Dual Bracewell interferometer. The modulation efficiency depends only on the nulling configuration, and is independent of wavelength.

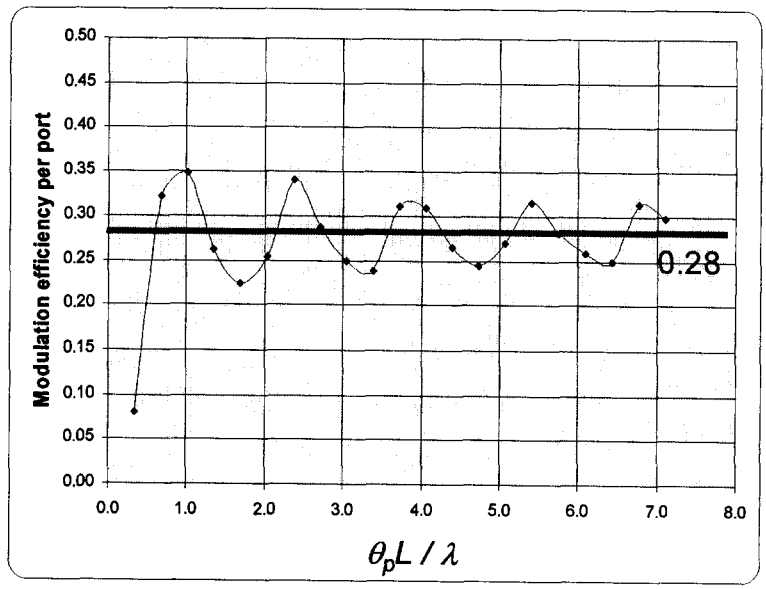


Figure 4

Will say something about all planet photons going to the detector if the configuration is phased up properly

### 3.1.4.2. Stellar leakage

Light from the star leaks through because the star has a finite extent and therefore would get through around even a perfect null and because the null is imperfect and has a finite floor. The photon rate due to stellar leakage is given by

$$S_{SL} = \tau\alpha \int_{\nu\min}^{\nu\max} \left(\Upsilon(\nu, L, \theta_*, \gamma, p) + \mathfrak{N}_{\text{floor}}\right) A_{ap}\Omega_* B_{ph}(\nu, T_*) \tag{1.8}$$

where

$\Omega_* = \pi\theta_*^2$ - solid angle subtended by the star

$A_{ap}$ – area of a single aperture

$B_{ph}(\nu, T) = \frac{2}{c^2}\frac{\nu^2}{\left[\exp\left(\frac{h\nu}{kT}\right)-1\right]}$ - Plank's distribution function in units of photons/m$^2$/sec/Hz/sr (check) (1.9)

$\mathfrak{N}_{\text{floor}}$ – null floor

$\Upsilon(\nu, L, \theta_*, \gamma, p) = \gamma \cdot \left(\frac{2\pi}{c}\nu L\theta_*\right)^p$ - leakage function. It connects the photon rate collected by a single aperture to the total stellar leakage photon rate for a given architecture. See ref. Charley. (1.10)

$\theta_* = 0.757\frac{\sqrt{\mathfrak{L}_*/\mathfrak{L}_{sun}}}{d_*^{(p\text{sec})} \cdot T_*^2}$ - angular radius of the star (radians)

$d_*^{(p\text{sec})}$ -distance to the star in parsecs

$T_*$ - temperature of the star (K)

$\mathfrak{L}_*/\mathfrak{L}_{sun}$ - relative luminosity of the star

p – null order of the given architecture, e.g. Dual-Chopped Bracewell p=2, Bow-tie p=4. see Table 1

$\gamma$ –architecture dependent leakage parameter, see Table 1

c – speed of light

L –array length

$\tau$ – internal throughput of the instrument. Includes optics losses and detector conversion efficiency

$\alpha = 1/N_{ap}$ – loss for the incoherent signal. Incoherent signal must be split between at least as many output ports as there are collecting apertures.

For the test case described in Figure TestCase the stellar leakage is X photo-electrons/second

This depends on array size, L. Point to Table 1 column X for leakage parameters

### 3.1.4.3. Local zodi

The LZ photo-electron rate is given by

$$S_{LZ} = \tau\alpha \int_{\nu\min}^{\nu\max} A_{tot}\Omega_{LZ}(\nu, D) B_{LZ}(\nu, T_{LZ}) d\nu \tag{1.11}$$

where $A_{tot}$ – total collecting area

$\Omega_{LZ}(\nu, D) = 1.4\left(\frac{c/\nu}{D}\right)^2$ - etendue ??? of a single telescope (reference) (1.12)

and BLZ is the local zodi brightness. The following parametric model was used to estimate the local zodi brightness, without having to do a full numerical integration of the Kellsall model.

$$B_{LZ}(\nu,\varepsilon) = \frac{\tau_{LZ,90}}{\sqrt{(\sin\varepsilon)^2 + \left(C_{LZ}\left(\frac{c/\nu}{\lambda_{0,LZ}}\right)^{\zeta}\cos\varepsilon\right)^2}} B_{ph}(\nu, T_{LZ}) \tag{1.13}$$

where $\tau_{LZ,90} = 4.0 \times 10^{-8}$, the optical depth towards the ecliptic poles

$\varepsilon$ - the ecliptic latitude

$C_{LZ} = 0.6$ determines how the optical depth increases towards the ecliptic plane

$\zeta = -0.4$ needed to match the shapes of the curves at the different wavelengths

$T_{LZ} = 265$ K is the effective temperature of the dust

The simple model is able to reproduce the local zodi contribution to the background predicted by SPOT.

### 3.1.4.4. Signal to noise and integration time.

The equations 1.5, 1.x, and 1.7 define quantities used in equation 1.4 and allow us to calculate the time required by a given configuration to obtain required SNR while looking at a canonical planet around a given star. For example: usual example, so many seconds.

### 3.1.4.5. Time available for observation, visits, single time obs. Limit.

The next step is to check if the required integration time is short enough to perform a meaningful search observation. The amount available for an observation of a single stellar system is limited by several factors. Assuming that the instrument is in orbit around the sun, the star is accessible only during a part of the year due to interferometer's FOR limitations with respect to anti-sun direction. The time during which the star is observable, $T_{obs}$, is given by

$$T_{obs} = \frac{T_{orb}}{\pi} a\cos\left(\frac{\cos(\theta_{FOR})}{\cos(\varepsilon)}\right) \tag{1.14}$$

where $\theta_{FOR}$ – field of regard half-angle

$\varepsilon$ – ecliptic latitude of the star

$T_{orb}$ – instrument orbital period around the sun (1 year)

To detect a planet a system must be observed several times ($N_{visits}$) and so one limit on the time available for a single observation is $T_{obs}/N_{visits}$, with $N_{visits}$ currently set at 3. Another limit is that we would like the planet to remain relatively stationary in its orbit during a single observation. Currently this time limit is defined to be $T_{single}$=7 days. The star is excluded from the list if

$T_{int} > \min(T_{single}, T_{obs}/N_{visits})$

### 3.1.4.6. and sorting procedure

At this point we have a list of stars with habitable zones that can be successfully examined by the interferometer configuration and we've calculated integration time required for an observation of each stellar system. The star list is subsequently arranged in the ascending order of integration time. Assuming the observations will be performed sequentially starting with the shortest integration time star, a cumulative time that adds $N_{visits}T_{int}$ for each star is calculated. Stars with the cumulative time below the time available for detection phase observations, $T_{search}$, are counted in the number of stars searched, $\mathcal{N}_d(L)$ and are stored in the *Searched* stars list.

The above procedure is repeated for various array lengths. The results for the test case architecture are shown in Fig. 5.

For configuration with a fixed array length one simply reads the number of stars searched at a

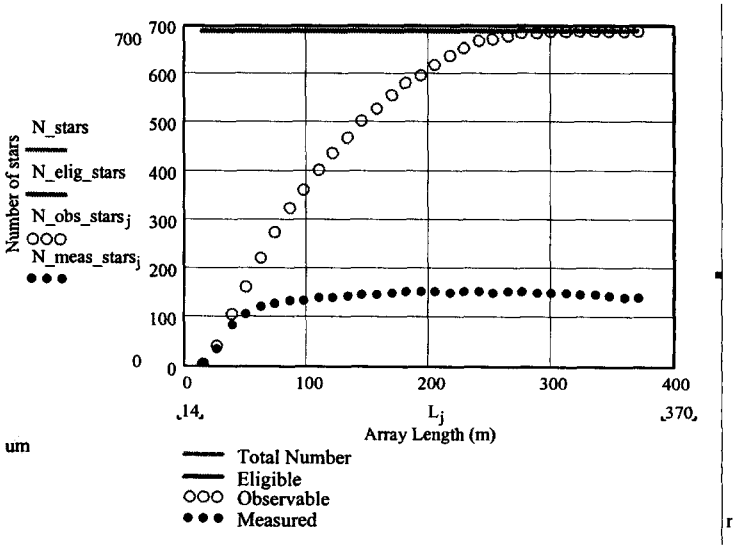


Figure. 5

given length. For example, a structure with L=40 will be able to observe $\mathcal{N}_d$= stars.

For a configuration with a variable array length the procedure is similar except that we assume that the array will be resized for each star to minimize needed integration time. It is these optimum integration times that arranged in the ascending order of integration times and the cumulative time calculated. For example the test case architecture with a variable L, but limited to Lmin(60m)<L<Lmax(375m), will be able to search $\mathcal{N}_d$= stars.

### 3.2. Spectroscopy

The number of planets that can be examined during the characterization phase of mission is calculated similarly to what was done for the detection phase. The differences are that for the spectroscopy calculation we used an optical bandwidth channel of $\lambda_1$=9.5 to $\lambda_2$=10 μm and the total available time cutoff was implemented as described in the following paragraph.

First consider the case where all stars have planets, i.e. $\eta_{earth}$ = 1. Starting at the top of the list with the shortest integration times, we proceed down the list, accumulating the integration time until we reach the total time available for spectroscopy, $T_{spec}$. The number of stars searched is denoted by $N_{s,all}(T_{spec})$. If instead $\eta_{earth}$ = 0.1, then, we only expect to do spectroscopy on 10% of the sources, but we don't know a priori which ones they will be – it won't be the first 10% of stars on the list with the shortest integration times. For this case we go down the list until the cumulative time reaches $T_{spec}$ / 0.1. The number of stars to this point is $N_{s,all}(T_{spec} / \eta_{earth})$, of which we expect to examine a fraction $\eta_{earth}$ with spectroscopy. Therefore, the time used for spectroscopy is again $T_{spec}$, but the number of stars examined is now

$$\mathcal{N}_{spec} = \eta_{earth} N_{s,all}\left(T_{spec}/\eta_{earth}\right) \tag{1.15}$$

If planets are rare and $\eta_{earth}$ is small, the initial list is long, the average distance for stars on the list is large, and the number of stars that can be examined with spectroscopy will be small.

## 4. COMPARISON OF NULLING ARCHITECTURES

The previous Section described our method for calculation of the number of stellar systems that can be searched during the planet detection phase of the mission, $\mathcal{N}_{det}$, and the number of planets that can be examined spectroscopicly during the characterization phase, $\mathcal{N}_{spec}$. The results are shown in Table 1. The configurations were compared assuming equal collecting area for each.

## 5. DISCUSSION

The $\theta^2$ configuration do better than $\theta^4$. This is contrarily to previous expectation. The reason is that the key figure of merit is how a long a configuration needs to integrate for to achieve a required SNR, or equivalently the SNR a configuration achieves in 1 second of integration.

The reason is that although the $\theta^4$ suppress the stellar leakage they also have much lower modulation efficiency. This occurs because they never completely phase up the signal, i.e. send all the planet photons to a detector, as the hi-res DCB does.

Figure 6 shows the plot of stellar distances vs. the required integration. The leakage dominates at near distances, but it does not matter much as the integration times are short. At longer distances, the noise is dominated by the local zodi and the leakage is less important, although still significant.

As can be seen from eq. 1.5. the SNR goes linearly with the signal, i.e. modulation efficiency, as square root of the stellar leakage. In other words, the modulation efficiency is much stronger factor.

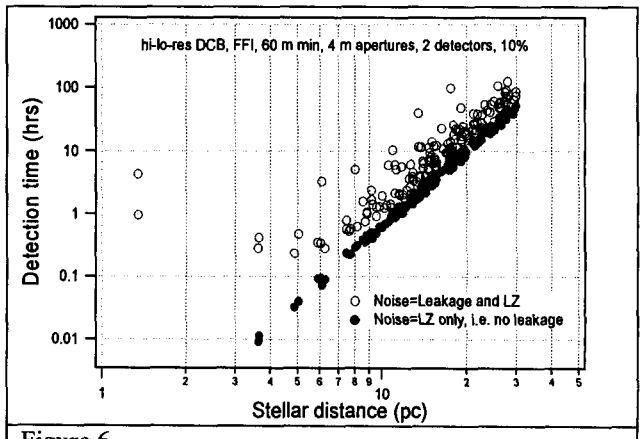

Figure 6

## 6. SUMMARY AND CONCLUSIONS

The $\theta^2$ configuration do better than $\theta^4$

Look for architectures that have high modulation efficiency.

The work described in this paper was performed at the Jet Propulsion Laboratory, California Institute of Technology, under contract with the National Aeronautics and Space Administration.

## 7. REFERENCES

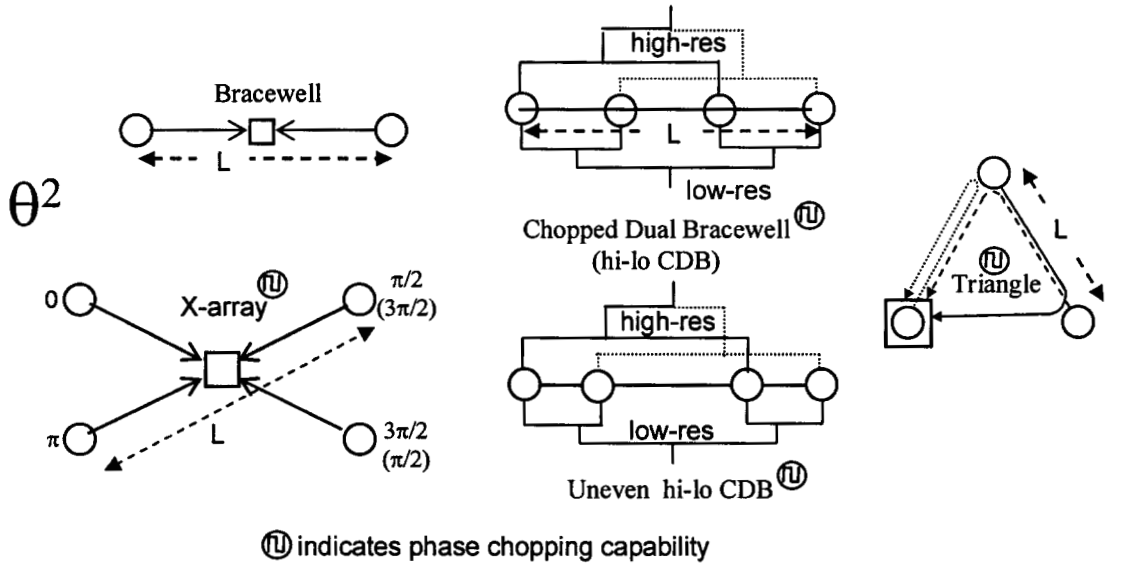


Figure 1:

| | | example | $\theta^2$ architectures | | | | $\theta^4$ | |
|---|---|---|---|---|---|---|---|---|
| | | DCB hi res | Uneven hi-lo DCB | hi-lo DCB | X-array 3:1 | Triangle | CDAC | Bow-tie |
| **Performance** | | | | | | | | |
| Detection Phase | $\mathcal{N}_d$ | | *84* | *224* | *206* | *181* | *124* | *120* |
| Characterization Phase | $\mathcal{N}_{spec}$ | | *8* | *14* | *10* | *18* | *12* | *12* |
| **Configuration Parameters** | | | | | | | | |
| Array length (meters) | L | 36 | 36 | var > 60 | var > 40 | var >20 | 40 | var > 60 |
| Modulation efficiency | $\eta_{mod}$ | 0.57 | 0.45/0.44 | 0.57/0.44 | 0.44 | 0.47 | 0.25 | 0.21 |
| null order | p | 2 | 2 | 2 | 2 | 2 | 4 | 4 |
| resolution parameter | $\chi_{res}$ | 0.75 | 0.67/0.56 | 0.75/1.17 | 1.58 | 0.68 | 1.1 | 1.1 |
| stellar leakage parameter | $\gamma$ | 0.22 | 0.28/0.03 | 0.22/0.06 | 0.05 | 0.38 | 0.002 | 0.002 |
| Collecting area (m^2) | $A_{tot}$ | 32.2 | 32.2 | 32.2 | 32.2 | 32.3 | 0.0 | 32.3 |
| Number of apertures | $N_{ap}$ | 4 | 4 | 4 | 4 | 3 | 4 | 6 |
| Apertures diameter (m) | $D_{ap}$ | 3.2 | 3.2 | 3.2 | 3.2 | 3.7 | | 2.62 |
| **Implementation Assumptions** | | | | | | | | |
| Inner Working Angle param. | $X_{IWA}$ | 1 | 1 | 1 | 1 | 1 | 1 | 1 |
| resolution wavelength | $\lambda_{res}$ | 10 μm | 10 μm | 10 μm | 10 μm | 10 μm | 10 μm | 10 μm |
| Sky coverage (+/- deg) | $\theta_{FOR}$ | 45 | 45 | 45 | 45 | 45 | 45 | 45 |
| Internal throughput | $\tau$ | 0.1 | 0.1 | 0.1 | 0.1 | 0.1 | 0.1 | 0.1 |
| Number of detectors | $N_{det}$ | 2 | 2 | 2 | 2 | 2 | 2 | 2 |
| Null floor | $\mathcal{N}_{floor}$ | 1.E-06 | 1.E-06 | 1.E-06 | 1.E-06 | 1.E-06 | 1.E-06 | 1.E-06 |
| Time avaliable for detection | $T_{search}$ | 1.5 yrs | 1.5 yrs | 1.5 yrs | 1.5 yrs | 1.5 yrs | 1.5 yrs | 1.5 yrs |
| Max single observation time | $T_{single}$ | 7 days | 7 days | 7 days | 7 days | 7 days | 7 days | 7 days |
| Time available for spectroscopy | $T_{spec}$ | 1.5 yrs | 1.5 yrs | 1.5 yrs | 1.5 yrs | 1.5 yrs | 1.5 yrs | 1.5 yrs |
| **Observation Parameters** | | | | | | | | |
| Planet radius | $R_p$ | $R_{Earth}$ | $R_{Earth}$ | $R_{Earth}$ | $R_{Earth}$ | $R_{Earth}$ | $R_{Earth}$ | $R_{Earth}$ |
| Planet temperature | $T_p$ | 260K | 260K | 260K | 260K | 260K | 260K | 260K |
| Inner habitable zone factor | $X_{INZ}$ | 0.7 | 0.7 | 0.7 | 0.7 | 0.7 | 0.7 | 0.7 |
| Required SNR | $SNR_{req}$ | 5 | 5 | 5 | 5 | 5 | 5 | 5 |
| Detection bandwidth (um) | $\lambda_1, \lambda_2$ | 7, 17 | 7, 17 | 7, 17 | 7, 17 | 7, 17 | 7, 17 | 7, 17 |
| Completeness | | | | | | | | |
| Number of visits | $N_{visits}$ | 3 | 3 | 3 | 3 | 3 | 3 | 3 |
| Orbit inclanation factor | $X_{incl}$ | 1.29 | 1.29 | 1.29 | 1.29 | 1.29 | 1.29 | 1.29 |

Table 1. parameters and performance